J|A|C|S
ARTICLES
Published on Web 06/21/2002

Topotactic Transformations of Sodalite Cages: Synthesis and NMR Study of Mixed Salt-Free and Salt-Bearing Sodalites

Henning Trill,[†] Hellmut Eckert,*[,†] and Vojislav I. Srdanov*[,‡]

Contribution from the Institut für Physikalische Chemie, Westfälische Wilhelms Universität Münster, Schlossplatz 7, 48149 Münster, Germany, and Center for Polymers and Organic Solids, University of California, Santa Barbara, California 93106

Received December 28, 2001

Abstract: A series of mixed sodalite samples, $Na_8[Al_6Si_6O_{24}]Br_x\cdot(H_3O_2)_{2-x}$, with the unit cell stoichiometries varying in the $0 < x < 2$ region, was made by hydrothermal synthesis and subsequently transformed into $Na_{6+x}[Al_6Si_6O_{24}]Br_x\cdot(4H_2O)_{2-x}$ and $Na_{6+x}[Al_6Si_6O_{24}]Br_x\cdot\blacksquare_{2-x}$ sodalites. Here, ■ refers to an empty sodalite cage. The three series, referred hereafter to as the Br/basic, Br/hydro, and Br/dry series, were characterized by powder diffraction X-ray and by ^{23}Na, ^{27}Al, and ^{81}Br magic angle spinning (MAS) NMR and high-resolution triple quantum (TQ) MAS NMR spectroscopy. We determined that incorporation of Br^- anions is 130 times more preferred than incorporation of $H_3O_2^-$ anions during the formation of sodalite cages, which permitted precise control of the halide content in the solid. Monotonic trends in chemical shifts were observed as a function of cage occupancy, reflecting continuous changes in structural parameters. A linear correlation between ^{81}Br chemical shift and lattice constant with a slope of −86 ppm/Å was observed for all three series. Likewise, ^{23}Na chemical shifts for Na^+ cations in salt-bearing sodalite cages correlate linearly with the lattice constant. Both results indicate a universal dependence of the ^{23}Na and ^{81}Br chemical shifts on the Na−Br distance. The ^{27}Al chemical shifts of Br/basic and Br/hydro sodalites obey an established relation between δ_{cs} and the average T−O−T bond angle of 0.72 ppm/°. Br/dry sodalites show two aluminum resonances, characterized by significantly different chemical shifts and quadrupolar interaction parameters. In that series, local symmetry distortions are evident from strong quadrupolar perturbations in the NMR spectra. P_Q values for ^{27}Al vary between 0.8 MHz in Br/basic sodalites and 4.4 MHz in the Br/dry series caused by deviations from the tetrahedral symmetry of the salt-free sodalite cages. For ^{23}Na, P_Q values of 0.8, 0.8, 2.0, and 5.7 MHz were found for sodium in bromo, basic, hydro, and dry cages, respectively. In addition, both ^{23}Na and ^{81}Br spectra offer some evidence that the Br^- anions in the Br/dry sodalite are displaced from the center of the expanded sodalite cage. For all three series, the spectral deconvolution of the ^{23}Na NMR line shapes permits an accurate determination of the mixed sodalite stoichiometry.

I. Introduction

The key characteristic of a solid solution A_xB_{1-x} ($0 \le x \le 1$) is the random distribution of its constituents A and B. For cubic lattices, the solid solution lattice parameter, a_o, is expected to obey Vegard's rule: $a_o = xa_o(A) + (x - 1)a_o(B)$. This rule is used as a convenient tool for determining the actual stoichiometry of the solid solution, while the deviations from it may indicate an onset of phase separation. In this study, we focus our attention to an unusual type of solid solution consisting of spatially separated molecular species inside sodalite cages whose interaction is mediated by the aluminosilicate framework. Because direct interaction between the molecular units is weak, such mixed sodalites differ from classical solid solutions. Nevertheless, it has been known that mixed sodalites with similar extraframework species obey Vegard's rule,[1,2] but may deviate from it when these species differ substantially from each other in size, even if their random distribution is preserved.[3] The ability of the sodalite lattice to host two incompatible species that otherwise would not form solid solutions on their own is unique and potentially important.

The sodalite lattice[4] is shaped by an aluminosilicate framework built from AlO_4 and SiO_4 tetrahedra that are slightly distorted due to small differences in the Si−O and Al−O bond lengths. The sodalite framework is flexible and can expand to

* To whom correspondence should be addressed. E-mail: srdanov@chem.ucsb.edu; eckerth@uni-muenster.de.
[†] Universität Münster.
[‡] University of California, Santa Barbara.

(1) Weller, M. T.; Wong, G. *Eur. J. Solid State Inorg. Chem.* **1989**, *26*, 619.
(2) Sieger, P. Ph.D. Thesis, University of Konstanz, 1992; p 139.
(3) Stein, A.; Ozin, G. A.; Stucky, G. D. *J. Am. Chem. Soc.* **1992**, *114*, 8119.
(4) Sodalite lattice is cubic (*P*43*n*) with the typical unit cell stoichiometry of $M_8[Al_6Si_6O_{24}]X_2$, where M is an alkali cation, and X is a monovalent anion. An example is naturally occurring chloro sodalite, $Na_8[Al_6Si_6O_{24}]Cl_2$, whose crystal structure was first solved by Pauling: Pauling, L. *Z. Kristallogr.* **1930**, *74*, 213. Note that sodalite unit cell occupies the volume of two sodalite cages. All three nuclei considered in this study (^{23}Na, ^{27}Al, and ^{81}Br) are at unique crystallographic sites thus yielding a single NMR signal in the case of a pure sodalite.

accommodate various extraframework species, which is accomplished by cooperative tilting of the framework tetrahedra about their 4-fold axes. An increase of this tilt angle contracts the sodalite lattice, which in turn decreases the Al−O−Si bond angles while leaving the O−T−O angles unchanged. Embraced by the framework are sodalite cages of ~6.5 Å in diameter, in which the extraframework species reside. Even though only three monovalent cations per sodalite cage are required for charge compensation of the negatively charged framework, an excess mineral salt unit, NaX, is typically incorporated in the synthesis. Inside the cages of such a salt-bearing sodalite, one finds a central anion surrounded tetrahedrally by four sodium cations. Salt-bearing sodalites are classified as feldspatoides[5] and are different from sodalites with no excess salt molecule present for which we propose the prefix salt-free.[6] Cages of salt-free sodalites contain up to four molecules of water,[7,8] for they are much closer to zeolites than to feldspatoides.[9]

As previously shown,[2,10] it is possible to synthesize mixed Br/basic sodalite with Br^- and $H_3O_2^-$ as central anions, which can be viewed as a solid solution of two ionic species supported by the sodalite framework. Using the same procedure[11] for transforming "basic" sodalite, $Na_8[Al_6Si_6O_{24}](H_3O_2)_2$,[12] into salt-free "hydro" sodalite, $Na_6[Al_6Si_6O_{24}]\cdot 8H_2O$,[13] and then into "dry" sodalite, $Na_6[Al_6Si_6O_{24}]$,[14] one can transform mixed Br/basic into Br/hydro and Br/dry sodalites without altering the bromine content.[3] The three mixed sodalites studied here are constructed from four different cages referred hereafter to as bromo, basic, hydro, and dry sodalite cages. As known from previous studies,[3,15,16] the random distribution of different extraframework species in mixed sodalites affects both the lattice parameters and the NMR resonances of the magnetic nuclei. NMR studies of sodalite solid solutions have largely concentrated on the ^{29}Si isotope[15] whose chemical shift is a sensitive measure of the average Al−O−Si bond angle in aluminosilicates.[17−20] In contrast, few studies have been devoted to nuclei with $I > {}^1/_2$ (^{27}Al, ^{23}Na, and ^{81}Br) in mixed sodalites whose NMR spectra are also sensitive to the structural changes.[3,16,21] The broken T_d symmetry of salt-free sodalite cages lowers the point symmetry of certain crystallographic sites in mixed sodalites, thus producing multiple sites and electric field gradients that perturb the NMR resonances of the quadrupolar nuclei. In the present study, we report on the preparation and characterization of Br/basic, Br/hydro, and Br/dry sodalite solid solution series, present extensive ^{23}Na, ^{27}Al, and ^{81}Br solid-state NMR data, and explore the informational content of NMR chemical shift and quadrupolar coupling parameters with respect to the structure, ion distribution, and other order/disorder phenomena.

II. Experimental Section

The synthesis of the Br/basic sodalites was carried out in Teflon-coated 40 mL stainless steel autoclaves. A desired amount (ranging between 6 and 15 mmol) of aluminum-isopropoxide (Aldrich: 22 940-7) and 0.36 mol of NaOH pellets (Aldrich: 30 657-6) free of carbon-dioxide impurity was topped off with 30 mL of distilled water and stirred until a clear solution was obtained. A known amount (between 0.5 and 40 mmol) of NaBr (Aldrich: 22 034-5) required for the bromine content desired in the mixed sodalite was added to the solution. After the solution was stirred for 15 min, the corresponding stoichiometric amount (6−15 mmol) of tetraethyl-orthosilicate (Aldrich: 33 385-9) was added to the solution. The autoclave was topped off with distilled water until 90% of its volume was occupied, closed tightly, and kept at 350 K for 10−20 days. After opening the containers, the highly basic solution above the sample was decanted, and the sodalite samples were washed (through a plastic membrane filter) to remove sodium hydroxide adhered to the crystal surfaces. Only 50 mL of deionized water was used for this purpose because the prolonged washing may extract NaOH from basic sodalite cages (see below). The samples of the Br/hydro series were obtained by stirring Br/basic sodalites in deionized water for several days. The pH of the suspension was kept at 6 ± 0.5 during extraction by frequent addition of diluted H_2SO_4. The washing process was terminated when the pH did not change significantly for a day, indicating a complete transformation of Br/basic sodalite into Br/hydro sodalite. The Br/dry sodalite samples were obtained by heating Br/hydro sodalites to 670 K under vacuum (~5×10^{-5} Pa) for 8 h.

X-ray diffraction powder patterns in the $12° < 2\theta < 6°$ region were taken with Cu Kα (1.54178 Å) radiation on a Scintag-X2 spectrometer in 0.02° steps and at a scanning rate of 2°/min. Silicon powder was used as an internal standard. The background correction, removal of the Bragg reflections due to the $K\alpha_2$ line, and the subsequent determination of the lattice constants by the least-squares fitting procedure were done with the DMSNT 1.37 software package from Scintag. The lattice constants were calculated from the corrected peak data to an accuracy of about 0.001 Å. The Br/dry samples were kept inside a hermetically closed beryllium cell during the data acquisition to avoid rehydration.

The thermogravimetric analysis (TGA) was carried out on a Netzsch 609 Simultaneous Thermal Analyzer. About 50 mg of sample was heated at 10 K/min from room temperature to 1373 K against a dry Al_2O_3 standard and background corrected. The weight loss between 383 and 800 K was ascribed to intracage water, while the weight loss below 383 K was attributed to surface water.

^{23}Na, ^{27}Al, and ^{81}Br MAS NMR spectra were obtained on a high-resolution Bruker DSX 500 NMR spectrometer, with a magnetic field of 11.7 T, at 132.26, 130.28, and 135.04 MHz, respectively. Complementary experiments were undertaken on Bruker DSX 400 and CXP 200 spectrometers to extract chemical shift and quadrupolar coupling parameters from field dependent data. 1 M aqueous solutions of $AlCl_3$, NaCl, and NaBr were used as chemical shift references. Typical spinning speeds ranged from 10 to 15 kHz. For all samples, simple one-pulse MAS NMR spectra were obtained with 30° pulses 1.0 μs long. High-resolution triple quantum (TQ) MAS NMR spectra were

(5) Breck, D. W. *Zeolite Molecular Sieves*; Wiley: New York, 1973.
(6) The term "salt-free" was first introduced by Barrer to distinguish between a "base-bearing" hydroxosodalite dihydrate and "salt-bearing" sodalites. Here we use the term "salt-free" for all sodalites without central anion.
(7) Engelhardt, G.; Felsche, J.; Sieger, P. *J. Am. Chem. Soc.* **1992**, *114*, 117.
(8) Latturner, S. E.; Sachleben, J.; Iversen, B. B.; Hanson, J.; Stucky, G. D. *J. Phys. Chem. B* **1999**, *103*, 7135.
(9) Zhdanov, S. P.; Buntar, N. N.; Egorova, E. N. *Dokl. Akad. Nauk SSSR* **1964**, *154*, 419.
(10) Barrer, R. M.; Cole, J. F. *J. Chem. Soc. A* **1970**, 1516.
(11) Barrer, R. M.; Cole, J. F. *J. Phys. Chem. Solids* **1968**, *29*, 1755.
(12) Hassan, I.; Grundy, H. D. *Acta Crystallogr.* **1984**, *C39*, 3.
(13) Felsche, J.; Luger, S.; Bearlocher, C. *Zeolites* **1986**, *6*, 367.
(14) Campbell, B. J.; Delgado, J. M.; Cheetham, A. K.; Iversen, B. B.; Blake, N. P.; Shannon, S. R.; Latturner, S.; Stucky, G. D. *J. Chem. Phys.* **2000**, *113*, 10226.
(15) Engelhardt, G.; Sieger, P.; Felsche, J. *Anal. Chim. Acta* **1993**, *283*, 967.
(16) Jelinek, R.; Chmelka, B. F.; Stein, A.; Ozin, G. A. *J. Phys. Chem.* **1992**, *96*, 6744.
(17) Engelhardt, G.; Radeglia, R. *Chem. Phys. Lett.* **1984**, *108*, 271.
(18) Jacobsen, H. S.; Norby, P.; Bildsoe, H.; Jakobsen, H. J. *Zeolites* **1989**, *9*, 491.
(19) Engelhardt, G.; Luger, S.; Buhl, J. C.; Felsche, J. *Zeolites* **1989**, *9*, 182.
(20) Johnson, G. M.; Mead, P. J.; Dann, S. E.; Weller, M. T. *J. Phys. Chem. B* **2000**, *104*, 1454.
(21) Jelinek, R.; Stein, A.; Ozin, G. A. *J. Am. Chem. Soc.* **1993**, *115*, 2390.

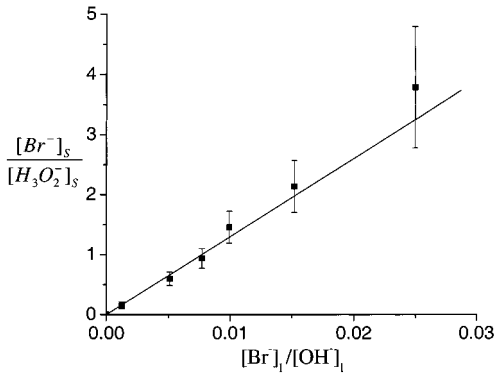

Figure 1. Experimentally determined concentration ratio of the two anions in the sodalite cages versus that in the precursor solution and the weighed least-squares fit to eq 2. The selectivity factor $K_{Br/OH} = 130 \pm 11$ is extracted from the fit.

acquired using a three-pulse sequence with zero quantum filtering.[22] For ^{27}Al TQ MAS, the first two hard pulses were 3.6 and 1.9 μs in length, respectively. The third selective 90° pulse had a length of 10 μs. A total of 64−128 free induction decays, containing 24−60 scans each, was acquired in the t_1 dimension. For ^{23}Na TQ MAS, the pulses were 4.0, 1.4, and 10 μs in length, respectively.

III. Results and Interpretation

A. Control of the Halide Content in Mixed Sodalites. The synthesis of bromo sodalite requires an extremely basic solution; hence, both Br^- and $H_3O_2^-$ anions compete for the inclusion into the growing sodalite lattice.

$$(Br^-)_l + (H_3O_2^-)_s \underset{k_{OH}}{\overset{k_{Br}}{\rightleftharpoons}} (Br^-)_s + (H_3O_2^-)_l \qquad (1)$$

where l and s denote the liquid and solid phases, respectively. Under equilibrium conditions, an equilibrium constant $K_{Br/OH}$ (selectivity factor) is given by

$$K_{Br/OH} = \frac{k_{Br}}{k_{OH}} = \frac{[H_3O_2^-]_l}{[Br^-]_l} \cdot \frac{[Br^-]_s}{[H_3O_2^-]_s} \quad \text{or}$$

$$\frac{[Br^-]_s}{[H_3O_2^-]_s} = K_{Br/OH} \cdot \frac{[Br^-]_l}{[H_3O_2^-]_l} \qquad (2)$$

Here $[Br^-]_s$ and $[H_3O_2^-]_s = 1 - [Br^-]_s$ are the fractional occupancies of sodalite cages by bromide and basic anions, respectively. From Figure 1, where $[Br^-]_s/[[H_3O_2^-]_s$ is plotted against $[Br^-]_l/[H_3O_2^-]_l$, a selectivity factor of $K_{Br/OH} = 130 \pm 11$ is extracted by a weighed least squares procedure. The selectivity factor, $K_{Br/OH}$, denotes how many times bromo cages are more likely to form than are basic cages during the synthesis of Br/basic sodalite. Although bromo cages are 130 times more preferred, a large excess of the halide source relative to the aluminum source is necessary to obtain a nearly pure bromo sodalite. Low initial halide concentrations coupled with a large selectivity factor lead to quick depletion of the Br^- anions from the solution, thus resulting in Br/basic sodalite crystallites with a large Br^- concentration gradient. To avoid such gradients, we purposely opted for small yields by utilizing large molar ratios of the extraframework to framework precursors. In this way, a sufficient reservoir of halide anions is provided to ensure a uniform sodalite composition.

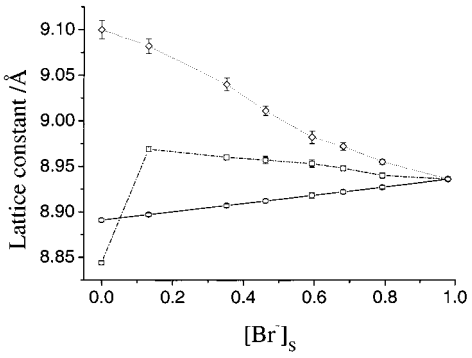

Figure 2. Variation of the lattice constant with the fractional occupancy of bromo cages, $[Br^-]_s$, for the Br/basic (solid line), Br/hydro (broken line), and Br/dry (dotted line) series.

The halide content of the Br/basic sodalite samples was determined by X-ray powder diffraction using the established Vegard's rule for this series.[2] The halogen contents of these samples in the Br/hydro and Br/dry solid solution series were taken as identical to those of the corresponding Br/basic samples from which they were prepared. For the Br/hydro series, the halide content was independently deduced by measuring the water content via TGA, assuming that hydro cages contain four molecules of water as they do in pure hydro sodalite.[13] A good agreement between the two methods supports the notion[3] that the bromine contents of the sodalites do not change during the course of the topotactic transformation from one type of solid solution to the other.

While Vegard's rule holds very well for Br/basic sodalites, consistent with the postulated random distribution of the two anions, a strong deviation exists in the Br/hydro series (see Figure 2). In this series, the cell constant increases steadily from 8.893 Å in the pure bromo sodalite to 8.969 Å in the sample with 90% hydro cages. However, the lattice constant drops to 8.844 Å for the pure hydro sodalite. The same effect has been observed in silver-exchanged sodium Br/hydro sodalites where the abrupt lattice contraction has been attributed to the occurrence of structural hydrogen bonding, which is suppressed in the presence of Br^- anions.[3] If Vegard's rule were obeyed throughout the entire Br/hydro series, the lattice constant of the pure hydro sodalite would have been 8.977 Å. Vegard's rule seems to hold for the Br/dry series too, although small deviations are visible. Note that the Br/dry sodalite with up to 90% of dry cages is cubic, but the pure dry sodalite is not. The departure from the cubic symmetry in pure dry sodalite is indicated by the occurrence of weak reflections outside the $P\bar{4}3n$ space group and the splitting of the main reflections due to orthorhombic distortion of the sodalite framework.[14,23]

B. NMR Spectroscopy. All of the nuclei examined within the present study have spin quantum numbers $I > {}^1/_2$ and moderately large nuclear electric quadrupole moments: $eQ(^{23}Na) = 10.89 \times 10^{-30}$ m^2, $eQ(^{27}Al) = 14.03 \times 10^{-30}$ m^2, $eQ(^{81}Br) = 27.6 \times 10^{-30}$ m^2. The effects of nuclear-electric quadrupolar interactions on the MAS NMR line shapes can be calculated using second-order perturbation theory resulting in anisotropic broadening and shifting of the central $|{}^1/_2\rangle \leftrightarrow$

(22) (a) Frydman, L.; Harwood, J. S. *J. Am. Chem. Soc.* **1995**, *117*, 5367. (b) Amoureux, J. P.; Fernandez, C.; Steuernagel, S. *J. Magn. Reson.* **1996**, *A123*, 116.

(23) Shannon, S.; Campell, B.; Metiu, H.; Blake, N. *J. Chem. Phys.* **2000**, *113*, 10215.

$|-1/2\rangle$ coherence. The resonance position is given by[24]

$$\delta_{exp} = \delta_{cs} + \delta_Q \quad (3)$$

where

$$\delta_Q(m) = -\frac{3}{40}\frac{I(I+1) - 9m(m-1) - 3}{I^2(2I-1)^2}\frac{P_Q^2}{\nu_0^2} = -D_I\frac{P_Q^2}{\nu_0^2} \quad (4)$$

ν_0 is the resonance frequency, and $P_Q = C_Q(1 + (\eta^2/3))^{1/2}$ is the quadrupolar coupling parameter with the quadrupolar coupling constant C_Q and the asymmetry parameter η. For the central $|1/2\rangle \leftrightarrow |-1/2\rangle$ coherence, the constant D_I only depends on the nuclear spin quantum number I and amounts to 6000 for spin $5/2$ nuclei such as ^{27}Al, and 25 000 for spin $3/2$ nuclei such as ^{81}Br and ^{23}Na.

According to eqs 3 and 4, the chemical shift and the quadrupolar shift contributions can be separated by measuring the spectra at two different Larmor frequencies: $\nu_0{}^\alpha$ and $\nu_0{}^\beta$. From the corresponding resonance shifts δ^α and δ^β, we can determine P_Q according to

$$P_Q^2 = \frac{1}{D_I}\frac{\delta^\alpha - \delta^\beta}{\left(\frac{1}{\nu_0^\beta}\right)^2 - \left(\frac{1}{\nu_0^\alpha}\right)^2} \quad (5)$$

Consequently, the isotropic chemical shift can be deduced as well by using eq 3.

Alternatively, these parameters can be obtained from triple quantum (TQ) MAS NMR. This method takes advantage of the fact that the angular dependence introduced by first-order quadrupolar coupling is the same for the $|1/2\rangle \leftrightarrow |-1/2\rangle$ and the $|3/2\rangle \leftrightarrow |-3/2\rangle$ coherences. Owing to this fact, the anisotropic second-order quadrupolar broadening can be removed by correlating these two coherences using standard 2-D NMR methodology. After a shearing transformation with appropriate scaling,[25] the projection of one (the F_2) dimension corresponds to the regular 1-D spectra, while the projection in the other (F_1) dimension is devoid of anisotropic broadening. The isotropic chemical shift, δ_{cs}, can be calculated from the shifts in the F_1 and F_2 dimensions, δ_{F1} and δ_{F2}:

$$\delta_{cs} = \frac{17\delta_{F1} + 10\delta_{F2}}{27} \quad (6)$$

C. ^{27}Al MAS NMR. In cubic sodalites with identical sodalite cages, aluminum has only one crystallographic site, located at the linkage of four adjacent sodalite cages. In mixed sodalites, however, the degeneracy of the aluminum site is removed, thus giving rise potentially to multiple environments associated with different cage occupancies.

Figure 3 shows the ^{27}Al MAS NMR spectra of the three solid solution series examined in this study. The ^{27}Al chemical shift and quadrupolar coupling parameter P_Q, as deduced from field dependent measurements and/or from TQMAS, are summarized in Table 2. In the case of the Br/basic sodalite series (Figure 3, column I), only a single resonance with a nearly symmetric line shape was found, whose full width at the half-maximum (fwhm)

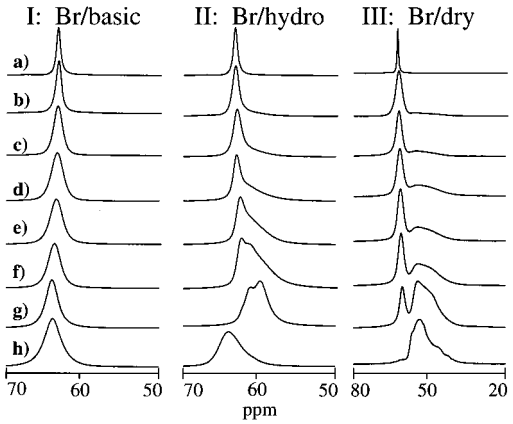

Figure 3. ^{27}Al MAS NMR spectra (observed at 130.28 MHz) of the Br/basic, Br/hydro, and Br/dry series. The percentage of bromo cages, identical for all three series within the same row, is as follows: (a) 98%, (b) 78%, (c) 67%, (d) 61%, (e) 45%, (f) 36%, (g) 10%, (h) 0%.

Table 1. Comparison of the Halide Content in the Br/basic and Br/hydro Series Determined by X-ray and TGA Methods

	X-ray: Br/basic		TGA: Br/hydro	
	a_0/Å	Br fract. (%)	Δm/%	Br fract. (%)
a	8.936	97.8	0.25	98.2
b	8.927	79.1	2.59	81.1
c	8.922	68.1	5.93	62.6
d	8.918	59.3	6.69	55.4
e	8.912	46.2	8.67	38.6
f	8.907	35.2	9.61	32.3
g	8.897	13.2	12.79	11
h	8.891	0	14.1	2.4

varies between 80 and 270 Hz. Evidently, the chemical shift differences between the various ^{27}Al sites are smaller than the inhomogeneous broadening caused by solid solution disorder; thus, no resolved resonances are detected. The ^{27}Al resonance in this series shifts linearly to higher frequencies (from 63.2 to 64.3 ppm) with a decrease in the Br^- content. As shown in Figure 2, the substitution of $H_3O_2^-$ by Br^- anions expands the sodalite lattice and thus increases the average Si−O−Al bond angle, which changes the isotropic chemical shift of the ^{27}Al resonance to more positive values (less deshielding), as discussed below. Simultaneously, P_Q remains unchanged at 0.8 ± 0.1 MHz in agreement with previous studies on the end-members of this series.[26,27] This indicates that the ion substitution does not alter significantly the electric field gradient (EFG) around the aluminum site, consistent with the fact that all sodalite cages in the Br/basic series contain a central anion and four Na^+ cations.

The ^{27}Al NMR spectra of the Br/hydro and Br/dry series in Figure 3 (columns II and III) display two distinct resonances that are more widely separated in the Br/dry series. The high-frequency resonance in both series is narrow and nearly symmetric, while the low-frequency resonance shows a marked shape asymmetry indicating strong second-order quadrupolar coupling. For sample II-f, variable temperature MAS NMR and ^{27}Al TQMAS NMR reveal only two aluminum sites, where P_Q values of 1.6 and 2.1 MHz are extracted for the high- and the low-frequency resonances, respectively. Note that both reso-

(24) Samoson, A. A. *Chem. Phys. Lett.* **1985**, *119*, 29.
(25) Engelhardt, G.; Kentgens, A. P. M.; Koller, H.; Samoson, A. *Solid State Nucl. Magn. Reson.* **1999**, *15*, 171.
(26) Mundus, C.; Muller-Warmuth, W.; Buhl, J. C. *Eur. J. Mineral.* **1996**, *8*, 231.
(27) Nielsen, N. C.; Bildsoe, H.; Jakobsen, H. J.; Norby, P. *Zeolites* **1991**, *11*, 622.

Table 2. Chemical Shift and Quadrupolar Coupling Parameters for ^{23}Na, ^{27}Al, and ^{81}Br in the Br/basic, Br/hydro, and Br/dry Series

	δ_{cs}/ppm						P_Q/MHz					
	Br/basic		Br/hydro		Br/dry		Br/basic		Br/hydro		Br/dry	
^{27}Al	site 1	site 2	site 1	site 2	site 1	site 2	site 1	site 2	site 1	site 2	site 1	site 2
a	63.4		63.4		63.4		0.8		0.8		0.8	
b	63.5		63.4		63.0		0.8		0.8		1.0	
c	63.7		63.2		63.0	59.6	0.8		0.9		1.3	4.3
d	63.8		63.2		62.6	59.9	0.8		0.9		1.3	4.4
e	63.9		63.0		62.5	59.2	0.8		1		1.5	4.4
f	64.0		62.8		62.2	59.1	0.8		1.2		1.5	4.4
g	64.3		62.4	62.4	61.5	58.1	0.8		1.6	2.1	1.4	4.1
h	64.5			65.6	0		0.8			2.2		
^{23}Na												
a	7.5		7.4		7.4		0.7		0.7		0.7	
b	7.8	3.4	7.3	−0.2	6.2		0.6	0.7	0.7	1.5	1	5.4
c	8	3.5	7.2	0	6		0.6	0.6	0.7	1.6	1.3	5.6
d	8.3	3.7	6.9	0.1	4.7		0.6	0.6	0.7	1.6	1.3	5.6
e	8.9	3.8	6.6	0	3.2		0.7	0.6	0.6	1.6	1.5	5.6
f	9.1	3.9	6.7	−0.3	2.6		0.7	0.6	0.6	1.6	1.6	5.6
g	10.2	4.6	6.4	−0.1	0.5		0.7	0.7	0.6	1.7	1.8	5.6
h		5		−0.1				0.8		1.1		5.6
^{81}Br												
a	−221.0		−221.0		−221.0		0.5		0.5		0.5	
b	−220.8		−221.2		−222.4		0.6		0.5		0.6	
c	−220.4		−221.8		−224.4		0.6		0.7		0.9	
d	−219.9		−223.3		−226.4		0.7		1.1		1.0	
e	−219.6		−225.4		−229.5		0.8		1.5		0.9	
f	−219.2		−227.1		−233.3		0.7		1.7		0.9	
g	−218.0		−230.6		−237.8		0.6		2.2		0.8	

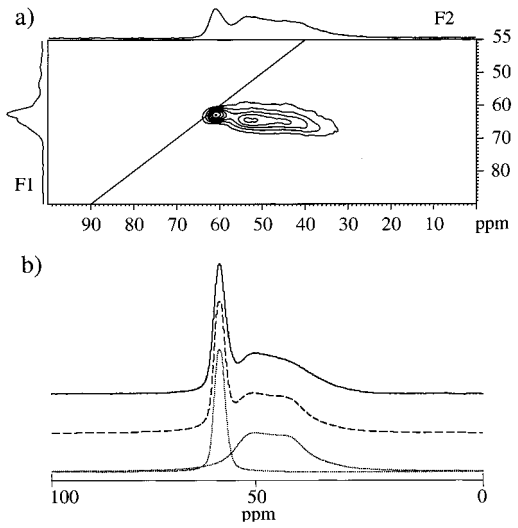

Figure 4. (a) ^{27}Al TQ MAS NMR spectra of the Br/dry sodalite sample with 36% bromo cages (sample III-f in Figure 3). (b) ^{27}Al MAS NMR spectrum of the same sample (solid line), the simulated spectrum (dashed line), and deconvolution of the two line components (dotted line). All spectra were observed at 104.22 MHz.

nances have the same chemical shift within the experimental error.

Figure 4a shows the ^{27}Al TQMAS spectrum of sample III-f from the Br/dry series where the two aluminum sites are clearly differentiated on the basis of their P_Q values. As we elaborate in more detail in the Discussion section, the very large P_Q value of the low-frequency resonance (4.4 MHz) indicates a substantial distortion of the tetrahedral aluminum environments in that series. Using the Hamiltonian parameters derived from this experiment, a satisfactory simulation of the MAS line shape can be achieved, as shown in Figure 4b. Both the MAS and the TQMAS results suggest the presence of a distribution of P_Q values thereby limiting the accuracy with which the average values can be determined.

To rationalize the existence of two distinct resonances in the Br/hydro and Br/dry series, it is necessary to consider the local aluminum environments. Aluminum atoms are bound to four oxygen atoms each linked to a sodium site in a different sodalite cage, which is always occupied if the cage is salt-bearing. If the cage is salt-free, however, the sodium site next to the aluminum-bound oxygen atom is vacant with a 25% probability. When the sodium site is unoccupied, the oxygen is likely to have a different local charge and may be slightly dislocated from its 24*i* site (see Discussion section for details). On the basis of these considerations and considering the compositional dependence of the spectra, we assign the high-frequency resonance to the aluminum atoms bound to four equivalent oxygen atoms, each linked to an occupied sodium site. Such an aluminum environment gives rise to rather small electric field gradients around the aluminum site, with P_Q values between 0.7 and 1.6 MHz as observed experimentally. The low-frequency resonances are assigned to aluminum environments associated with one vacant sodium site. Statistically, a distribution of zero to four vacant sodium sites would be expected. In contrast, we find only two aluminum resonances in both the Br/hydro and the Br/dry series, indicating that each aluminum has no more than one vacant neighboring sodium site. Indeed, the peak areas associated with these two aluminum sites are in excellent agreement with values predicted from the composition on the basis of a binary distribution. This is also consistent with the conclusions from a recent structure refinement of pure dry sodalite.[14,23] The lattice structure revealed that the sodium ions are strictly ordered, such that each aluminum site is linked to only one unoccupied sodium site.

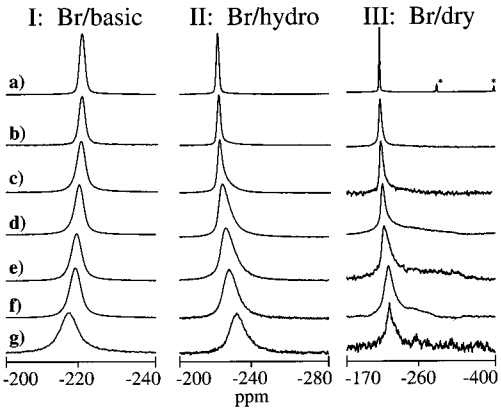

Figure 5. ^{81}Br MAS NMR spectra (observed at 135.04 MHz) of the Br/basic, Br/hydro, and Br/dry series. The percentages of bromo cages are the same as in Figure 3. Spinning sidebands are marked by asterisks.

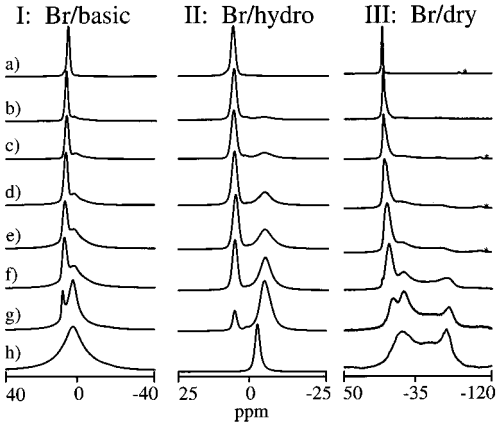

Figure 6. ^{23}Na MAS NMR spectra (observed at 132.26 MHz) of the Br/basic, Br/hydro, and Br/dry series. The percentages of bromo cages are the same as in Figure 3. Spinning sidebands are marked by asterisks.

D. ^{81}Br MAS NMR. The mixed sodalites considered in this study are expected to have only one bromine site where the Br^- anions are coordinated by four Na^+ cations in a tetrahedral geometry. For the Br/basic series, this is confirmed by the ^{81}Br MAS NMR spectra (Figure 5-I), which show only a single resonance. The ^{81}Br P_Q values scatter around 0.6 ± 0.2 MHz, reflecting only weak quadrupolar coupling in this series. Nevertheless, the random distribution of the two anions in the Br/basic series produces some disorder, as revealed by line broadening effects due to distributions of chemical shifts and/or P_Q values for each sample. The ^{81}Br isotropic chemical shift decreases linearly with the decrease of the bromine content, ranging from −221 to −217.5 ppm (see Table 2). Samples of the Br/hydro series (Figure 5-II) also have single peak ^{81}Br spectra, but the chemical shift variation with bromine content is opposite to that in the Br/basic series, reaching $\delta_{cs} = -226$ ppm at the lowest Br content. Concomitantly, the P_Q values increase from 0.5 to 2.2 MHz.

The ^{81}Br MAS NMR spectra of Br/dry sodalites (Figure 5-III) show one dominant resonance with isotropic chemical shifts between −220.4 and −235.8 ppm. While the P_Q values for this series are small and increase only slightly with a decrease in the bromine content (0.6−0.8 MHz), there is a dramatic increase in the resonance line width (from 250 to 2400 Hz at 11.7 T). Furthermore, samples having bromine contents below 70% display complex asymmetric line shapes, where the low-frequency side of the resonance extends up to −350 ppm. While such spectroscopic features are indicative of strong quadrupolar coupling, the excessive broadening suggests a wide distribution of interaction parameters precluding a more detailed analysis with simulation routines.

E. ^{23}Na MAS NMR. Within the solid solution series studied, Na^+ cations occur in four different environments. Sodium cations in bromo cages are coordinated by three framework oxygen atoms and one bromine anion. In basic cages, Na^+ cations are surrounded by the three framework oxygen atoms and one extraframework oxygen. According to low-temperature crystallographic data on pure basic sodalite, this extraframework oxygen, a part of the $H_3O_2^-$ anion, is separated from the Na^+ cation by 2.4 Å.[7] In hydro cages, sodium is surrounded by three framework oxygen atoms at a distance of about 2.5 Å and three (out of four) water molecules at similar distances.[7] Finally, sodium cations in dry sodalite cages are coordinated by the three framework oxygen atoms at a distance of 2.35 Å and three additional atoms from the same six ring at distances of about 2.95−3.05 Å. Unlike bromo cages, dry sodalite cages do not have tetrahedral symmetry. The absence of the central anion in those cages creates a large electric field gradient at the sodium site, as documented by quadrupolar line shapes of the NMR resonances of the corresponding sodium cations (see below).

Table 2 summarizes the ^{23}Na lineshape parameters for the various sodium sites in the three solid solution series. The ^{23}Na MAS NMR spectra of the Br/basic series are presented in Figure 6-I. Generally, two distinct resonances can be identified; the peak at around 9 ppm is assigned to sodium ions in bromo cages, whereas the peak at around 4 ppm stems from the sodium ions in basic cages. Some of the spectra show a low-frequency shoulder near −3 ppm, which is attributed to sodium ions in hydro cages that have resulted from the partial extraction of NaOH units during the washing procedure. The ^{23}Na NMR spectrum of the Br/basic sodalite sample containing 98% Br^- anions (sample I-a) is characterized by a chemical shift of 7.5 ppm and a P_Q of 0.7 MHz, in good agreement with the literature.[27] For lower bromine contents, the determination of P_Q values by the two-field method becomes more difficult owing to extensive peak overlap. Nevertheless, approximate P_Q values of 0.7 ± 0.1 and 0.6 ± 0.2 MHz can be estimated for ^{23}Na sites in bromo and basic cages, respectively.

The ^{23}Na MAS NMR spectra of Br/hydro sodalites in Figure 6-II show two resonances assigned to sodium in bromo and hydro cages, whose line shapes are well separated from each other. The resonances from sodium cations in hydro cages are characterized by P_Q parameters between 1.5 and 1.7 MHz, as determined by both the two-field method and TQ MAS NMR (see Figure 7a). For pure hydro sodalite, we obtain $\delta_{cs} = 0 \pm 0.1$ ppm and $P_Q = 1.1 \pm 0.1$ MHz.

The ^{23}Na NMR spectra of the Br/dry sodalites (Figure 6-III) show two line-shape components. The component between 5 and 0 ppm is assigned to sodium cations in bromo cages. Its line width increases from 210 to 1500 Hz with a decrease of the bromine content reflecting an increase in P_Q values from 0.7 to 1.8 MHz. The MAS line shapes, recorded at 52.9 MHz in this series, reveal a strong peak asymmetry indicating a superimposed distribution of P_Q values for this site (data not shown). The second line-shape component, characterized by strong second-order quadrupolar broadening effects, is attributed to sodium ions located in dry cages. The corresponding line

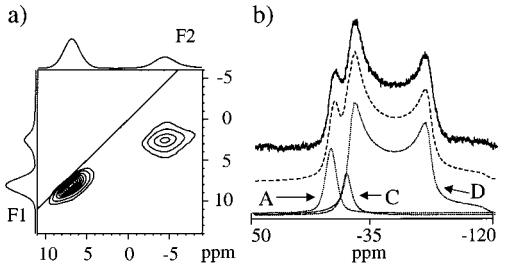

Figure 7. (a) ^{23}Na TQ MAS NMR spectrum of the Br/hydro sodalite sample with 36% bromo cages. (b) Spectra of the Br/dry sodalite sample with 10% bromo cages (solid line), simulated spectrum (dashed line), and deconvoluted line-shape components belonging to sodium in A, bromo cages; C, hydro cages; and D, dry cages (dotted line). All spectra were observed at 132.26 MHz.

shape can be simulated with quadrupolar coupling constants between 5.4 and 5.8 MHz and asymmetry parameters close to zero (see Figure 7b). These results are consistent with values previously published for pure dry sodalite (P_Q = 5.9 MHz).[28]

IV. Discussion

There are two different aspects of the solid solution effects in mixed sodalites addressed in this study. The first concerns the monotonic changes in the structural (lattice) parameters, which affect chemical shifts of the NMR resonances of both the framework and the extraframework species within each series. Most of the previous studies were predominantly focused on the relationship between the change in the structural parameters and NMR spectra of the framework nuclei. The second aspect of the solid solution effects concerning the electric field gradients produced by the disorder is much less explored, which gives rise to additional sites and/or amplified nuclear electric quadrupolar interactions. We discuss both of these aspects for all three solid solution series, considering both the effects on the framework and the local environments of the extraframework ions.

A. Solid Solution Effects on the Framework. When the water molecules are removed from the cages of hydro sodalite, the sodalite framework expands rather than contracts (see Figure 2). Similarly, the lattice of salt-free sodalite is expanded in comparison with that of salt-bearing sodalites.[29] The underlying reason for this unusual behavior is the Coulomb repulsion between the charge compensating alkali cations. In the absence of the central anion or some polar molecular species such as water, the unscreened Coulomb repulsion pushes the alkali cations away from the center of the sodalite cage. This in turn increases the average Al−O−Si bond angle leading to lattice expansion. Because of the unusually large Al−O−Si bond angles, the aluminosilicate framework of dry sodalite is strained and eager to absorb small atoms or molecules that can help screen Coulomb repulsion.

The above considerations can help rationalize the observed trends in the lattice parameters of mixed sodalites shown in Figure 2. In the Br/basic series, Coulomb repulsion between sodium cations is screened in both cages, which allows lattice contraction to the point required to accommodate the two different central anions. Contrary to this, in the Br/dry series there is an apparent competition between two opposing forces. Coulomb repulsion is efficiently screened in bromo cages, thus allowing for their contraction, but not in dry cages, hence favoring their expansion. The repulsive forces prevail in this series for the whole lattice expands monotonically as the bromine content decreases. The trends in the lattice parameters of the Br/hydro series are more complex. The Coulomb repulsion of the sodium cations in hydro cages appears to be screened to some extent, yet repulsive forces prevail so that the Br/hydro lattice expands slightly with the decrease of the bromine content. It appears that such a trend persists for the entire solid solution series except at its very end where the lattice of hydro cages suddenly shrinks. The reasons for such a behavior are uncertain at present. A possible explanation invokes long-range hydrogen bonding, which is disrupted by a small percentage of bromo cages.[3] However, we found the chemical ^{1}H MAS NMR shifts of 10% Br-containing Br/hydro and that of pure hydro sodalite to be 4.5 and 4.3 ppm, respectively, indicating insignificant differences in hydrogen-bonding strengths between the two samples. Alternatively, the water coordination in the hydro cages of Br/hydro sodalite may differ from that in pure hydro sodalite. The attractive interaction between water molecules and sodium ions in adjacent sodalite cages[30] can also contribute to the sudden contraction of the sodalite lattice if the remaining small percentage of bromo cages can influence the water configuration in the hydro cages. Different water configurations competing for the ground state of hydro sodalite were recently proposed by Shannon et al.[31]

The sodalite framework expansion is accompanied by an increase in the average T−O−T bond angle, for which the correlations with ^{29}Si and ^{27}Al chemical shifts have been established.[17−20] In the case of sodalites, the average Al−O−Si bond angle can be calculated from the lattice constant, a_o, using the following expression:[32]

$$\alpha = \frac{180^\circ}{\pi} \arccos\left(\frac{\overline{\mathrm{SiO}}}{2\overline{\mathrm{AlO}}} + \frac{\overline{\mathrm{AlO}}}{2\overline{\mathrm{SiO}}} - \frac{a_o^2}{16\overline{\mathrm{SiO}}\cdot\overline{\mathrm{AlO}}}\right) \quad (7)$$

Assumed here are rigid TO_4 tetrahedra with the following interatomic distances: Al−O = 1.742 Å, Si−O = 1.612 Å, O−O = 2.871 and 2.701 Å for AlO_4 and SiO_4 tetrahedra, respectively. As the Al−O−Si bond angle increases with an increase of the lattice constant, the degree of s-hybridization in the oxygen orbitals of the T−O bonds changes accordingly. This leads to a higher effective electronegativity of the oxygen and therefore an increased deshielding of the T atoms (high-frequency shifts).[33] In the present study, linear correlations between δ_{cs} and the Al−O−Si bond angle are found for all three mixed sodalite series (Figure 8). The slopes of the Br/basic and Br/hydro sodalite solid solution series are −0.71 and −0.69 ppm/°, respectively, in close agreement with the literature value of −0.72 ppm/° found for several halogen sodalites.[18] Unlike the situation in the Br/hydro series, samples of the Br/dry series show two distinct ^{27}Al resonances, characterized by different chemical shifts and quite different P_Q values (1.4 and 4.4 MHz). For these resonances, the slopes in the plot of

(28) Koller, H.; Engelhardt, G.; Kentgens, A.; Sauer, J. *J. Phys. Chem.* **1994**, *98*, 1544.
(29) The lattice constant of dry sodalite is 9.102 Å, while that of sodium chloro, bromo, and iodo sodalite is 8.870, 8.893, and 9.012 Å, respectively.
(30) Shannon, S. R.; Metiu, H. *J. Phys. Chem. B* **2001**, *105*, 3813.
(31) Shannon, S. R.; Blake, N. P.; Metiu, H. J., unpublished data.
(32) Hassan, I.; Grundy, H. D. *Acta Crystallogr.* **1984**, *B40*, 6.
(33) Radeglia, R.; Engelhardt, G. *Chem. Phys. Lett.* **1985**, *114*, 28−30.

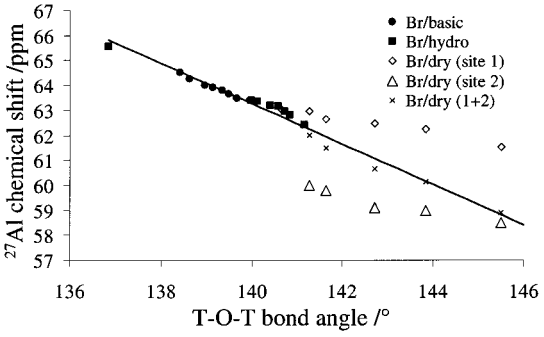

Figure 8. ^{27}Al MAS NMR chemical shift versus average Si−O−Al bond angle calculated from the lattice constant for all three series (see text for details).

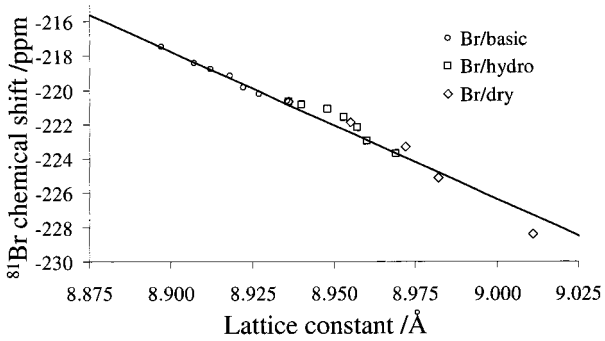

Figure 9. ^{81}Br MAS NMR chemical shift versus lattice constant. Data points from the spectra in Figure 5-III-f and 5-III-g are omitted due to the large experimental errors.

chemical shift versus average Al−O−Si bond angle are significantly smaller than those for the other series (see Figure 8).

The P_Q values of the various aluminum sites were simulated on the basis of a point charge model,[28] using an electric quadrupole moment of 14×10^{-30} m^2 and a Sternheimer antishielding value of −2.3 for the ^{27}Al nucleus.[34] While this model is more suited for ionic environments, it has been shown for other nuclei[35,36] that such an approach is capable of mimicking the effect of electron density distribution in bonding orbitals within the first coordination sphere. The adjustable parameter in this procedure is the effective charge on the oxygen atoms, reflecting the polarity of the Al−O bonds. To reproduce the experimental value of $C_Q = 0.7$ MHz in bromo sodalite, the oxygen charge had to be adjusted to −1.6e in these calculations. Because of the covalent nature of the Al−O bond, this value is far from −0.67e that can be derived in ionic systems following the procedure by Brown and Altermatt.[37] This discrepancy shows the limitations of the point charge model; yet we find this simple model is useful in comparing relative magnitudes of quadrupolar coupling constants for the different aluminum sites. Following the predictions of Brown and Altermatt,[37] the charge of oxygen next to a vacant sodium site in Br/hydro sodalite was increased by −0.3e to account for the missing Na−O bond. This resulted in a C_Q value of 2 MHz in good agreement with the experiment.

To simulate $P_Q = 4.4$ MHz of the ^{27}Al site linked to the vacant sodium site in Br/dry sodalite, one of the four Al−O−Si bond angles was expanded by 22°. This was accomplished in our simple model by keeping the original orientation of the Al−Si vector while increasing the average Al−O−Si bond angle of the aluminum site by about 5.5°. Within the sodalite lattice, such an operation requires dislocation of the T atoms from their crystallographic sites, which affects other T−O−T but also O−T−O bond angles. According to Vogel et al.,[38] the change in the O−Si−O bond angle affects only the chemical shift anisotropies, but not the isotropic values. Projecting these findings to the ^{27}Al NMR shifts in our system, we propose that the chemical shift difference between the two Al sites in the Br/dry series arises from differences in the average Si−O−Al bond angles. In this case, the 3.3 ppm difference in chemical shift observed for the two ^{27}Al resonances corresponds to a difference of about 4.5° in average Al−O−Si bond angles of the two sites. This is in reasonable agreement with the difference in average T−O−T angles (5.5°) deduced from the analysis of the quadrupolar interactions. The smaller slopes observed in Figure 8 for each site within the Br/dry series suggest that these angles change only slightly. For this series, the main compositional effect concerns the population ratio of these sites. The universal correlation of chemical shift with the average Al−O−Si bond angle is still obeyed, however, only if the average shift of both sites, weighed by their population ratio, is plotted.

B. Solid Solution Effects on the Extraframework Species. Figure 9 reveals a universal correlation of the ^{81}Br chemical shift with the lattice parameter a_o with a slope of −86 ppm/Å for all three solid solution series. On the basis of the dominance of the paramagnetic deshielding term in the Ramsey expression for chemical shifts, high-frequency ^{81}Br shifts imply increased Na−Br wave function overlap due to covalency. Thus, the observed trend can be linked to changes in the Na−Br internuclear distance, which can be derived from the lattice constant using the model of Hassan and Grundy.[32] Here, a constant Na−O distance of 2.35 ± 0.01 Å is postulated in agreement with previous studies.[32,39] The unusually wide range of Na−Br distances deduced from this model (2.75 to 3.1 Å) is consistent with the large changes in chemical shifts observed experimentally, yielding −35 ppm/Å. Note that the largest Na−Br distances are expected at the low bromine concentrations in the Br/dry series where the expanded bromo sodalite cage becomes much larger than required by the bromine anion. The P_Q values of the ^{81}Br resonances in the Br/hydro series are significantly larger than in the two other series indicating a distortion of the tetrahedral symmetry, most likely caused by dislocation of the sodium anions. This may be triggered by an attractive interaction between sodium atoms and water molecules in the neighboring cages, still under investigation in our laboratories.

The cause of the relatively large ^{81}Br line widths in the spectra of these samples is more difficult to explain, considering that the Br$^-$ anions populate sites with T_d symmetry. The quadrupole moment of ^{81}Br is larger than those for the other nuclei studied here, which makes its NMR resonances more sensitive to structural perturbations. Also, it is conceivable that the Br$^-$

(34) Lucken, E. A. C. *Nuclear Quadrupolar Coupling Constants*; Academic Press: London and New York, 1969.
(35) Townes, C.; Dailey, B. *J. Chem. Phys.* **1949**, *17*, 782.
(36) Jellison, G. H.; Panek, L. W.; Bray, J. P.; Rouse, G. B. *J. Chem. Phys.* **1977**, *66*, 802.
(37) Brown, I. D.; Altermatt, D. *Acta Crystallogr.* **1985**, *B41*, 244.
(38) Vogel, C.; Wolff, R.; Radeglia, R. *Collect. Czech. Chem. Commun.* **1993**, *58*, 1255.
(39) Wiebke, M.; Engelhardt, G.; Felsche, J.; Kempa, P. B.; Sieger, P.; Schefer, J.; Fischer, P. *J. Phys. Chem.* **1992**, *96*, 392.

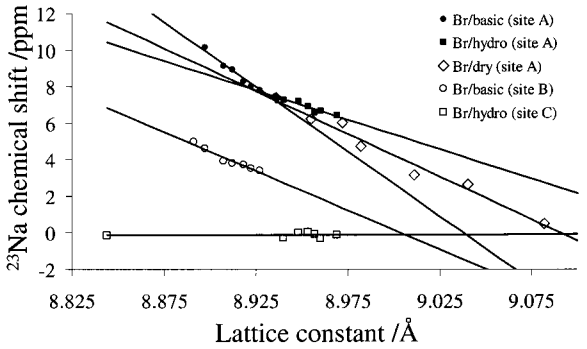

Figure 10. ^{23}Na MAS NMR chemical shift versus lattice constant for all three series. The experimental data for sodium cations in dry cages of the Br/dry series are not presented due to a large experimental error.

anions in enlarged bromo cages do not reside in the center of the sodalite cage, a situation similar to rare earth ions in endohedral fullerenes.[40] The EFG is the smallest in the center of the sodalite cage, but rises sharply elsewhere. A displacement of the Br^- anions from the center of the sodalite cages would therefore lead to strong quadrupolar effects, which are expected to increase with increased cage size, in agreement with the experimental findings.

The ^{23}Na chemical shifts as a function of lattice constant for the three solid solution series are shown in Figure 10. The trends observed can be discussed in terms of the four fundamentally different sodium environments mentioned earlier. As Figure 10 illustrates, sodium cations in bromo cages show a linear correlation of the ^{23}Na chemical shift with the lattice constant. Recent calculations by Tossell showed that the ^{23}Na shielding interaction is dominated by the paramagnetic term.[41] Hence, for these sodium sites, the observed trends in the chemical shift can again be linked to changes in the Na−Br distances. A decrease in Na−Br distance will lead to high-frequency shifts as a result of increased covalency. The slope of −70 ppm/Å with respect to the lattice constant (or −28 ppm/Å with respect to the Na−Br distance) measured for the Br/basic solid solution series agrees well with that in mixed halide sodalites observed recently in our laboratories.[42] We also found a linear correlation of the ^{23}Na chemical shift with the lattice constant for sodium in bromo cages of the Br/hydro and Br/dry series, albeit with somewhat different slopes. The spread in Al−O−Si bond angles encountered in the latter series, however, makes it more difficult to extract Na−Br distances from the lattice constants.

For sodium in basic cages of the Br/basic sodalite series, an analogous linear trend is observed. The systematic offset in the chemical shift arises from the replacement of Br^- by $H_3O_2^-$ anions in the first coordination sphere, whose deshielding contribution is smaller as compared to that of Br^- anions. Also, the variation of the chemical shift with the lattice constant (−43 or −17 ppm/Å with respect to the Na−anion distance) is significantly smaller than that for sodium in bromo cages.

For sodium in hydro cages, no obvious correlation between the lattice parameters and the chemical shift is observed. The chemical shifts near 0 ppm reflect a coordination environment similar to that of a hexaquo complex. In contrast to the sodium environments in other cages, sodium ions in hydro cages are octahedrally coordinated with six oxygen atoms, three of which belong to the framework oxygen and the other three to water molecules. This sodium environment is not expected to change much with lattice parameters, consistent with the ^{23}Na chemical shift behavior. For Br/dry sodalites, the chemical shift of sodium in dry cages scatters between −3 and 5 ppm and can only be determined within an error of a few ppm.

The point charge model discussed earlier was used to calculate the ^{23}Na quadrupolar coupling constants (P_Q) from the structural data. The point charges have been determined following the procedure by Brown and Altermatt,[37] resulting in −0.67e, −0.90e, −1.30e, and −0.89e for framework oxygen, oxygen in H_2O, oxygen in $H_3O_2^-$, and bromide anion, respectively. Using the ^{23}Na nuclear electric quadrupole moment of 11×10^{-30} m^2 and a Sternheimer antishielding value[34] of −4.1, quadrupolar coupling constants of 0.6, 0.7, 2.0, and 5.5 MHz were calculated for sodium sites in bromo, basic, hydro, and dry cages, respectively. This is in very good agreement with the experimental data in Table 2. We note that the variations of electric field gradients with lattice parameters in this series are generally small, while the increase of P_Q values for sodium in bromo cages of the Br/dry series with decreasing Br^- content is noticeable and cannot be explained simply by the distance change. It is possible that the sodium ions in salt-bearing cages of Br/dry sodalites are dislocated from the center of their six rings, as in the case of pure dry sodalite.[23] It is also possible that the Br^- anions are displaced from the center of the sodalite cages. Because the observed field gradients can be produced by a large variety of structural arrangements, no specific structural information can be extracted from the experimental data.

Finally, we note that the ^{23}Na NMR spectra also provide a convenient gauge of the sample chemical composition. We find that the bromine content in mixed sodalites determined from sodium NMR data is in good agreement with the more traditional methods listed in Table 1. The ^{23}Na MAS NMR signal of the sodium cations in bromo cages is well separated from the sodium resonance in hydro cages. By choosing a small ($\pi/6$) flip angle and sufficiently large relaxation delay times ($t > 5$ s), the fractional areas of both resonances in Figure 6-II can be used for accurate determination of the bromine content. The values need to be adjusted for the sodium cage content because bromo cages contain four sodium cations, while hydro cages have only three of them.

V. Conclusion

We have presented a comprehensive NMR study of three sodalite solid solution series, which can be transformed from one to another by topotactic manipulation of their extraframework species. Although data obtained on some specific individual sample compositions appear scattered in the literature, the present work has produced a number of inclusive experimental results and new insights. The determination of the selectivity factor for Br/basic sodalite series, $K_{Br/OH}$, enables synthesis of mixed sodalites with a desired accurate halide content. The realization that the halide content in mixed sodalites can be analyzed by using ^{23}Na MAS NMR spectroscopy is also new. Solid solution effects have a pronounced influence both on the aluminosilicate framework and on the local environments of extraframework ions, which can be followed in detail by the

(40) Takata, M.; Umeda, B.; Nishibori, E. *Nature* **1995**, *377*, 46.
(41) Tossell, J. *Phys. Chem. Miner.* **1999**, *27*, 70.
(42) Trill, H.; Eckert, H.; Srdanov, V. I., to be published.

compositional evolution of solid-state NMR chemical shift and quadrupolar interaction parameters. In particular, we find that the Na−Br distances are determined by the solid solution composition, producing linear correlations of the ^{23}Na and ^{81}Br chemical shifts with the lattice constant.

The NMR resonances are inhomogeneously broadened, owing to local fluctuations in the isotropic chemical shifts and electric field gradients. Topotactic removal of NaOH from the sodalite cage, followed by dehydration, produces large distortions of the framework tetrahedra resulting in the appearance of two significantly different aluminum sites, as evidenced by ^{27}Al chemical shift and quadrupolar interaction parameters. This indicates that the sodium vacancies are not statistically distributed within the cages but ordered in a way that each aluminum atom is linked to only one such site. That the tetrahedron-edge-length distortions are an important means of releasing strains in sodalite framework imposed by geometrical constraints has been first recognized by Depmeier.[43] In addition to this, ^{23}Na and ^{81}Br NMR results suggest that the Br^- anion in the Br/dry series may be displaced from the center of the cage, resulting in significant quadrupolar coupling effects.

The system we have studied is subject to further investigations. Our preliminary results show that the salt-free cages in the Br/dry sodalite can be doped with sodium, which converts them into sodalite cages with F-centers. Such a system would allow us to expand our studies, currently restricted to electro sodalites,[44] to presently unknown magnetically coupled F-center spin glasses.

Acknowledgment. We would like to thank Professor G. D. Stucky for help with the X-ray characterization, Dr. J. Chan and Dr. J. Hu for their support with the TQ MAS NMR, and Dr. H. Koller for valuable discussions. We also thank Dr. P. Sieger and Miss L. Damjanovic for their help at the initial stages of this project. This work was supported in part by the U.S. National Science Foundation (DMR-9520970) and the Wissenschaftsministerium Nordrhein-Westfalen.

JA012765S

(43) Depmeier, W. *Acta Crystallogr*. **1984**, *B40*, 185−191.

(44) Srdanov, V. I.; Stucky, G. D.; Lippmaa, E.; Engelhardt, G. *Phys. Rev. Lett.* **1998**, *80*, 2449.